Article

Body Condition and Allometry of Free-Ranging Short-Finned Pilot Whales in the North Atlantic

Patricia Arranz [1,*], Fredrik Christiansen [2], Maria Glarou [3], Shane Gero [2,4], Fleur Visser [5,6,7], Machiel G. Oudejans [5], Natacha Aguilar de Soto [1] and Kate Sprogis [8]

[1] Biodiversity, Marine Ecology and Conservation Research Group, Department of Animal Biology, Edaphology and Geology, University of La Laguna, 38200 Tenerife, Spain

[2] Section for Zoophysiology, Department of Biology, Aarhus University, Aarhus C, 8000 Aarhus, Denmark

[3] Húsavík Research Centre, University of Iceland, 641 Húsavík, Iceland

[4] Department of Biology, Carleton University, Ottawa, ON K1S 5B6, Canada

[5] Kelp Marine Research, 1624 Hoorn, The Netherlands

[6] Department of Freshwater and Marine Ecology, Institute for Biodiversity and Ecosystem Dynamics, University of Amsterdam, 1090 Amsterdam, The Netherlands

[7] Department of Coastal Systems, NIOZ, Royal Netherlands Institute for Sea Research, 1790 Den Burg, The Netherlands

[8] Great Southern Marine Research Facility, The UWA Oceans Institute, School of Agriculture and Environment, The University of Western Australia, Albany 6009, Australia

* Correspondence: arranz@ull.edu.es

Abstract: To understand the effects of anthropogenic disturbance on the nutritional health of animals, it is important to measure and understand the morphometrics, allometrics, and body condition of the species. We examined the body shape, allometric relationships, and body condition of short-finned pilot whales (*Globicephala macrorhynchus*) in three locations across the North Atlantic. Using unmanned aerial vehicles, the body length (BL) and width (along the body axis) were measured from photographs of the dorsal side, while body height (dorso-ventral distance) was measured on the lateral side. Seventy-seven pilot whales were measured (mean ± SD), including 9 calves (BL 2.37 m ± 0.118), 31 juveniles (2.90 m ± 0.183), and 37 adults (3.72 m ± 0.440). The body shape was similar among reproductive classes, with the widest point being anterior of the dorsal fin (at 30–35% BL from the rostrum). The cross-sectional body shape of the whales was flattened in the lateral plane, which increased towards the peduncle and fluke. The rostrum-blowhole distance and fluke width increased linearly with BL. The estimated volumes of pilot whales ranged between 0.15 and 0.32 m^3 for calves, 0.25 and 0.64 m^3 for juveniles, and 0.46 and 1.13 m^3 for adults. The body condition (residual of log-volume vs. log-length) ranged from −34.8 to +52.4%. There was no difference in body condition among reproductive classes or locations.

Keywords: morphometrics; unmanned aerial vehicles; unmanned aerial systems; aerial photogrammetry; *Globicephala macrorhynchus*; odontocete

1. Introduction

Body condition is a measure of the energy reserves of an animal relative to its structural size (e.g., length), and provides a valuable metric in individual and population health assessments [1,2]. Body condition has been related to survival and reproductive success both in terrestrial [3,4] and marine mammals [5–8]. In cetaceans, the body condition of individuals has been used to (1) assess and monitor the health of the population, (2) inform fluctuations in prey abundance [9], (3) monitor the health of individuals over anomalous climatic periods [10], (4) compare the health status of populations affected by different stressors [11], and (5) assess impacts from anthropogenic disturbances [12]. Body condition can also provide information about the reproductive potential of females [13,14]. For example, poor body condition makes it less likely for females to conceive [7]. Furthermore,

the body condition of pregnant females affects the size of the foetus, where females in poorer body conditions reduce energetic investment in their foetus [15,16]. Moreover, the body condition of the mother affects the growth of the calf, where shorter, thinner females are unable to invest as much energy into their young [17].

In the marine environment, the body condition of free-ranging individuals can be assessed through several methods, including blubber measures (thickness and lipid content), body composition (relative fat content), and body morphology (for a review see [18]). In terms of body morphology, the length, width and height of individuals can be calculated through photogrammetry methods [19–21]. Traditionally, aerial photogrammetry has been conducted from manned aircrafts [22,23]; however, more recently, quadcopter unmanned aerial vehicles (UAVs) have been used to assess the body condition of marine mammals [21,24]. Aerial photogrammetry can be used to capture images of the dorsal (length and width) and dorso-ventral (height) side of free-ranging individuals, and this approach has been applied for southern right whales (*Eubalaena australis*) [25], humpback whales (*Megaptera novaeangliae*) [26], gray whales (*Eschrichtius robustus*) [10], and sperm whales (*Physeter macrocephalus*) [27]. These measures can be applied to calculate the body volume of an individual, where 3D models are used to accurately represent the body shape of a species [25,28]. The approach using UAVs is non-invasive, cost-effective, and can be used on free-ranging cetacean populations from land- or boat-based platforms. The advancement of UAV technology and aerial photogrammetry methodology on smaller odontocetes has led to more in-depth bioenergetic questions being addressed, such as determining the pregnancy status in common bottlenose dolphins (*Tursiops truncatus*) [29], understanding the link between body condition and prey in killer whales (*Orcinus orca*) [30], and inferring the rapid loss in the condition of pygmy killer whales (*Feresa attenuata*) during stranding events [12].

Short-finned pilot whales (*herein* pilot whales) are distinctly shaped delphinids with an average size of approximately 3.6–4.7 m in females and males, respectively [31]. Coastal populations of pilot whales exist off the Canaries [32], Japan [33], Madeira [34], California, Hawaii [35], and across the Caribbean [36,37]. Furthermore, there appear to be distinct morphometric forms and genetic divergence within the species. At least three divergent morphotypes exist, two in the North Pacific and one in the North Atlantic [38,39]. In the North Pacific, the 'Naisa' or southern and smaller form and the "Shiho" or northern and larger form are segregated geographically and genetically apparently due to differences in sea surface temperature [39]. Across the North Atlantic, short-finned pilot whales DNA-sampled within the Caribbean (the Antilles and Florida), the east coast of the US (Carolina), and Spain (the Canaries) have been matched to pertain within the same genetic population [38,40]. Data from short-finned pilot whale mass standings recorded on the west and east coasts of the North Atlantic suggest that the Atlantic form is comparable in body length to the 'Naisa', the smaller form of the North Pacific [41,42].

Pilot whale females mature around nine years of age, lactate for three years on average, and calve a single offspring every five to eight years [43]. The known maximum lifespan is 60 years for females, who remain in the group as post-reproductive for decades [44]. To feed, pilot whales perform an energetic foraging tactic, in which they sprint (>9 m/s swimming speed) at >1000 m depth to chase large mesopelagic squid (Architeuthids) [45]. Anthropogenic disturbances in the marine environment (i.e., vessel noise) can disrupt the behavioural budget of this species, where noise disturbance reduces communication [46] and resting and nursing rates [47]. The alteration of critical resting periods when the pilot whales are at the surface (which are needed to recover from deep foraging dives) can potentially have negative effects on the foraging performance and energy balance of individuals [45]. Additionally, pilot whales are one of the most common species targeted by the whale-watching community globally, including the United States, Falkland Islands, the Antilles (i.e., off the coasts of Belize, Bermuda, Bahamas, Guadeloupe, and Dominica), the Azores, the Canaries, Japan, Philippines, and Tonga (Hoyt, 2001).

Anthropogenic disturbances on animals can affect the health of individuals. To understand the effects of anthropogenic disturbances on the health of animals, it is first necessary to measure the morphometrics, allometrics, and body condition of the species. The aim of this study was to assess body morphometrics, allometric relationships, and the body condition of short-finned pilot whales in the North Atlantic. To do this, UAVs were used to obtain measurements of pilot whales at three study locations in the North Atlantic (Tenerife, the Canaries; Terceira, the Azores; and Dominica, the Lesser Antilles).

2. Materials and Methods

2.1. Study Area and Species

UAV photogrammetry data on pilot whales were collected off the Canaries (off Tenerife in 2021 and 2022), the Lesser Antilles (off Dominica in 2017), and the Azores (off Terceira in 2018 and 2021) (Figure 1). In these three locations, data collection was performed in accordance with relevant guidelines and regulations. Off Tenerife, the UAVs were operated under a UAV Operator licence (Register # 2020064914) and an Advanced certificate of aircraft piloted by remote control (RPA20605OT and RPA20605OP) under the Spanish Aviation Safety and Security Agency (AESA). The research was conducted under a research permit from the Spanish Ministry for the Ecological Transition and the Demographic Challenge (permit AUTSPP/41/2020). In Dominica, research was undertaken under permit #RP16-04/88FIS-9 in 2016 and #RP17-08/12FIS-1 from the Fisheries Division of the Ministry of the Blue and Green Economy of the Government of Dominica. Off Terceira, research was conducted under permit LMAS-DRAM/2018/01 in 2018 and LMAS-DRAM/2021/04 in 2021.
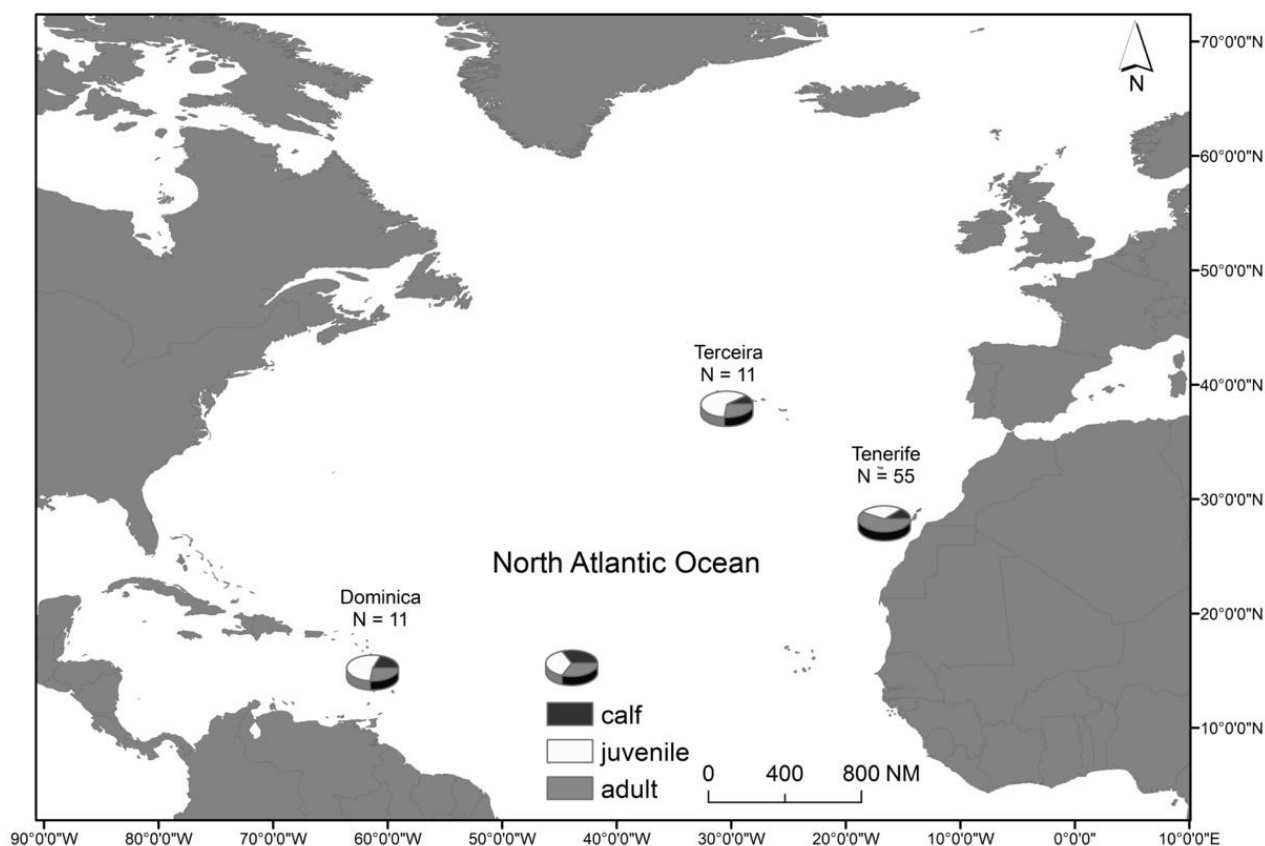

Figure 1. Map of the three study locations across the North Atlantic of short-finned pilot whales across Dominica (the Lesser Antilles), Terceira (the Azores), and Tenerife (the Canaries) with the proportion of sampled short-finned pilot whales within each reproductive class.

Off Tenerife, pilot whales comprise a resident reproductive population of approximately 250 individuals that are mostly observed on the leeward side of the island [48]. Photographs of the animals off Tenerife were taken between 13 February and 5 August 2021 and 1 April and 11 May 2022 (summer, winter). Off Terceira, pilot whales are regular visitors with a transient presence during the warmest months of the year [49]. Photographs of the animals off Terceira were taken on 4 August 2018 and 8 July 2021 (summer). Off Dominica, pilot whales are common and widely distributed year-round [50]. Photographs of the pilot whales were taken off Dominica on 23 April 2017 (spring).

Due to the common presence of short-finned pilot whales off these locations, the species was identified as short-finned pilot whales (based on genetics and morphology), and not their sister species the long-finned pilot whale (*Globicephala melas*). In the North Atlantic, long-finned pilot whales may have some marginal overlap in distribution with short-finned pilot whales; however, they typically inhabit cold temperate waters [51]. Off the Canaries, long-finned pilot whales have an extralimital presence [35,52], and there has been no stranding recorded of long-finned pilot whales from 2000 to 2017 (N = 540 stranded individuals, 12 species) [53], further supporting their presence in the area as unlikely. Similarly, sightings of the long-finned pilot whale off the Azores are sporadic, with only a few observations reported in the literature [54], supporting the classification of sampled specimens in different locations as the short-finned pilot whale.

2.2. Data Collection: Measuring Pilot Whale Morphometrics

To conduct aerial photogrammetry, two types of UAV quadcopters were used: A DJI Inspire 1 Professional (Tenerife and Dominica) and a DJI Phantom 4 Professional (Terceira). The Inspire had a Zenmuse X5 camera recording 4K video, 3840 × 2160, 25 fps equipped with a 25 mm f1.8 low-distortion lens in Tenerife, and a 15 mm lens in Dominica. The Phantom had a 20-megapixel camera recording 4K video, 4096 × 2160, 30 fps with an 8.8 mm f2.8 lens. Flight altitude ranged from 13–60 m (Tenerife: mean 38.36 ± 6.41 m; Terceira: 23.38 ± 6.67 m; Dominica: mean 15.10 ± 3.72 m). Calibration of the gyro sensors of the UAVs was conducted on land before data collection. Data were collected in good weather conditions (<3 Beaufort Sea state, no precipitation). The UAVs were launched and retrieved by hand by a researcher at the stern or bow of the research vessel. The distance between the UAV and the vessel was always <400 m to provide a clear line of sight of the UAV. The UAV operator had a screen (iPad 6th gen) on the controller, which allowed for a live feed to accurately position the UAV above an individual pilot whale. When hovering above the pilot whales, videos were recorded when the UAV was vertical above a pilot whale with the camera facing directly down (90°). Videos were recorded when a pilot whale was swimming (slowly swimming and resting) at the surface and the pilot whale was positioned directly in the centre of the frame (to account for any curvature of lenses). To avoid duplicate sampling of the same individuals, all still frames of animals from a given group were taken from the same flight. Each flight was <15 min in duration (the duration of one battery).

2.3. Data Processing of UAV Photographs to Extract Morphometric Values

Video recordings from the UAV were processed in the opensource software VLC (https://www.videolan.org) by one analyst (PA). During post-processing, three still frame photographs of the dorsal side of each pilot whale were extracted from the videos as jpegs. Dorsal photographs required the individual to have a straight body axis that was non-arching and where the body contours were clearly visible (Figure 2; see Christiansen et al., 2016). If the whale rolled 90° during sampling, a still frame of the dorso-ventral side was extracted. Each photograph was quality graded, based on posture, clarity, and contrast, following the protocol of [17], and only photographs of good quality were included in analyses.
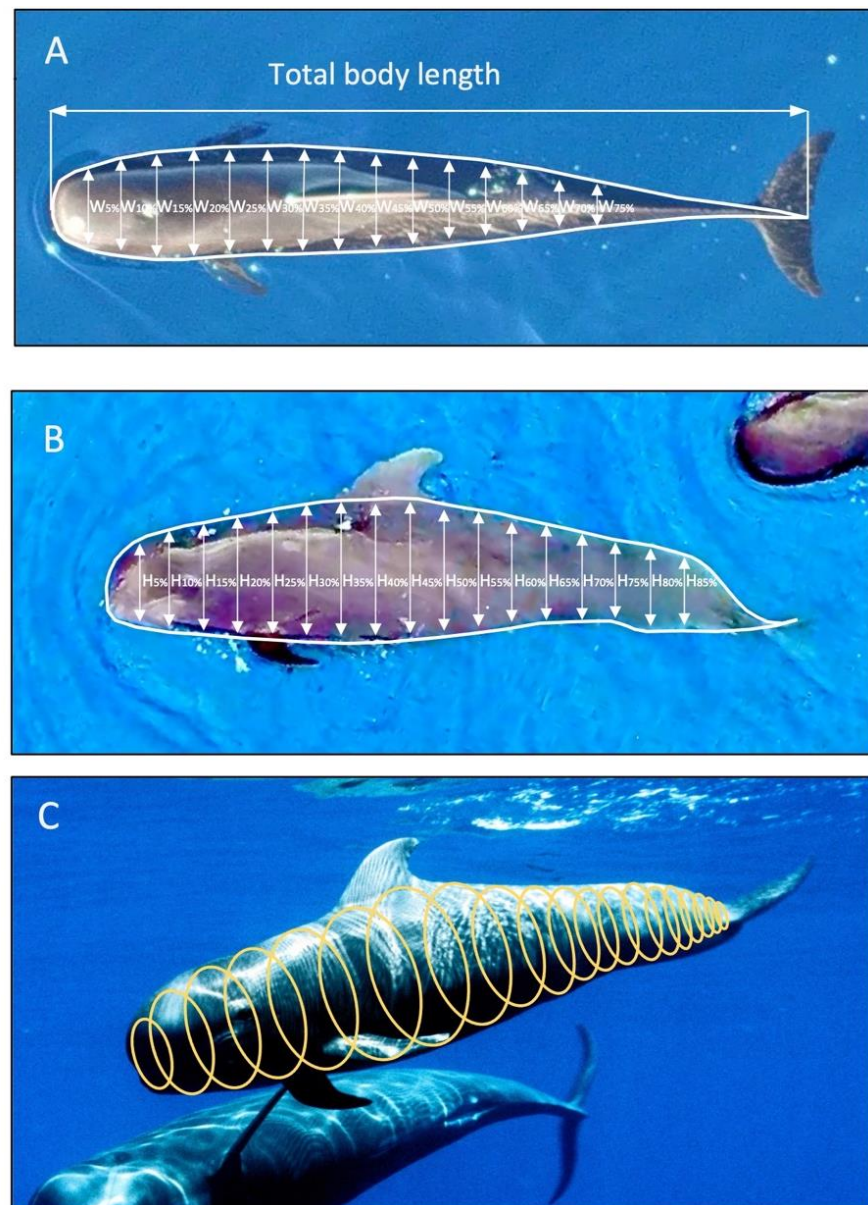
Figure 2. (**A**) Example aerial photographs of the dorsal surface of a pilot whale, used to measure body length (BL) and width (W) at 5% increments along the body axis from 5% to 85% body length from the rostrum to the fluke notch (white arrows). Additional measurements included the length from the rostrum to blowhole, and fluke width (tip of fluke extremities). (**B**) Dorso-ventral side of a pilot whale, used to extract body height (H) along the same measurement sites as used for width. (**C**) Cross-section along the transverse plane of the pilot whales to examine body shape and use infinite ellipses in modelling body volume for the body condition index.

For each dorsal photograph, the body length (BL, rostrum to fluke notch distance) and width (W) of the whales (at 5% increments along the body) were measured, in pixels, using a custom-written script in *R* v.4.2.1 ([20], R Core Team 2020) (Figure 2A). For the dorso-ventral photographs, the body height (H, dorso-ventral length) was measured, in pixels, for the same measurement sites [25] (Figure 2B). To examine allometric relationships with BL, additional measurements included the length from the rostrum to the blowhole, and fluke width (length between the tip of fluke extremities). All measurements were converted from pixels to meters using the known altitude of the UAV (measured with a LightWare SF11/C laser range finder, https://lightwarelidar.com/ (accessed on 01 April 2017), the camera focal length and sensor size, and the image resolution (see [17] for details). When

the laser range finder was not available, in Tenerife in 2021, the scaling of the photographs and the absolute measurements of the pilot whales was performed using photographs of the research vessel as a scale, which were captured at the same altitude as the pilot whale videos (for details of this scaling method, see [20]). To correct for the vessel altitude above the surface of the water, an item of known length was recorded floating on the water next to the vessel and three still photographs were extracted to measure the pixels of the object and the vessel. The difference between the actual and estimated vessel length using the known size object was used to correct each whale measurement (1.01% absolute length). All pixel measurements (stick, vessel, and whales) were performed with the free image processing software Paint.net (https://www.getpaint.net/ (accessed on 14 February 2021). The length of the vessel was then used to scale the photographs of the pilot whales from 2021 off Tenerife.

2.4. Classification of Reproductive Classes

A reproductive class was allocated to each pilot whale based on its BL, with animals < 2.5 m classified as calves, animals ≥ 2.5 m and <3.2 m classified as juveniles, and animals ≥ 3.2 m classified as adults [31]. The juvenile reproductive class was determined based on the known thickness of the growth layers in postnatal dentine (which is disproportionally larger before weaning, during the first and second years of age) and the existing conversion curves of age to length for females and males from the North Pacific 'Naisa' short-finned pilot whale population [31]. Pilot whales exhibit marked sexual dimorphism, where males are, on average, one meter longer than females (Table 1). Due to different maturation rates for females and males, females mature at 3.2 m in length and males at 4.2 m in length [31]; however, in this study, the sex of individual whales was not confirmed, and adults were not sexed, unless a dependent calf was present.

Table 1. Life history parameters for short-finned pilot whales from Kasuya and Matsui [31], corresponding to the North Pacific 'Naisa' form encountered off Japan, comparable in body length to the North Atlantic form, for which life history parameters are not available.

Life History Parameters	North Pacific 'Naisa' Morphotype
Max. length (female–male)	4.05–5.80 m
Max. weight	800–2300 kg
Weight at birth	37 kg
Length at birth	1.4 m
Length at weaning	2.5 m
Length at functional sexual maturity (female–male)	3.2–4.2 m

2.5. Body Shape, Allometrics, and Body Condition Analyses

To describe the body shape (morphometrics) of the pilot whales, the body measurements from the UAV photographs were used to calculate the (1) relative body width along the body axis and (2) the shape of the whales at transverse cross-sections. To calculate relative body width, the mean relative body widths of the whales were plotted against their BL from the rostrum to the notch in the fluke. To further describe the body shape of the whales and obtain a more representative shape, we examined the cross-sections in the transverse plane, and calculated the height:width (HW) ratio for each width and height measurement site (Figure 2) and plotted this ratio against the BL (for more details, see [25]). To examine how measurements change with size, the allometric relationships between BL and measurements from the rostrum to the blowhole, and fluke width, were plotted as scatter plots in absolute and relative values.

To measure the body condition of pilot whales, we used length, width, and height data. The relative body condition (BC_i) was calculated using volumetrics for each pilot whale i using the formula of [17]:

$$BC_i = \frac{BV_{obs,i} - BV_{exp,i}}{BV_{exp,i}} \tag{1}$$

where $BV_{obs,i}$ is the observed (measured) body volume of whale i, in m^3, and $BV_{exp,i}$ is the expected body volume of whale i, in m^3, given by the log–log relationship between body volume and body length (BL):

$$\log(BV_{exp,i}) = \alpha + \beta_1 \times \log(BL_i) \tag{2}$$

The BV_{obs} of each whale i was estimated from the sum of the volume of each body segment ($BV_{s,i}$) by modelling each segment s (the body section between two adjacent width measurements) as a series of infinitesimal ellipses (Figure 2) (Christiansen et al. 2019):

$$BV_{obs,i} = \sum_{s=1}^{20} BV_{s,i} \tag{3}$$

where BV_s is given by:

$$BV_{s,i} = BL_i \times 0.05 \times \int_0^1 \pi \times \frac{W_{A,s,i} + (W_{P,s,i} - W_{A,s,i}) \times x}{2} \times \frac{H_{A,s,i} + (H_{P,s,i} - H_{A,s,i}) \times x}{2} dx \tag{4}$$

where $W_{A,s,i}$ and $H_{A,s,i}$ are the anterior width and height measurements of body segment s for individual i, and $W_{P,s,i}$ and $H_{P,s,i}$ are the posterior width and height measurements of segment s for individual i, respectively. To account for the gradual decrease in height and width towards the rostrum and tail of the animal, the segments closest to the rostrum (0–5%BL from the rostrum (hereafter '%BL')) and the end of the tail region (85–100% BL) were modelled as elliptical cones [25]. Ellipses were used here since the cross-sectional shape of the pilot whales is more elliptical than square shaped (squircle), used in the latest published 3D model of pilot whales [28]. The authors of the study acknowledged that the 3D model required modifications to make the tail more elliptical rather than square shaped (squircle), therefore it was not used for calculations at this stage. Ellipses were suitable for short-finned pilot whales as pilot whales are laterally compressed in the fluke stock region [55]. Furthermore, ellipses and elliptical cones have been used previously to model the volume of humpback whales [26], gray whales [10], right whales [25], and sperm whales [27]. Once the body condition (BC_i) was calculated, a positive value signalled a relatively better condition than the average whale, whereas a negative value signalled a relatively poorer condition than the average whale.

2.6. Effects of Reproductive Class and Location on Body Condition

The effect of reproductive class and location on pilot whale body condition were investigated using linear models (LMs) in *R*. Model validation tests included scatter plots of residuals vs. fitted values and against each explanatory variable (to determine homogeneity of variance), histograms of residuals (to determine the normality of variance), and estimates of leverage and Cook's distance (to determine influential points and outliers, respectively). No violation of the assumptions of the LMs was found.

3. Results

3.1. Summary Statistics

A total of 258 measurements of pilot whales were obtained between 2017 and 2022 in three locations, representing 87 individuals. Individual raw length measurements, picture quality scores, and width measurements can be accessed from the Research Data Repository

of the University of La Laguna (DOI: 10.17632/5nhx7tgrxc.1x). After data filtering based on quality, a total of 77 measurements of individual whales remained (Table 2). The sex of the pilot whales was unknown, apart from lactating females with a dependent calf (N = 6 Tenerife, N = 3 Terceira, N = 2 Dominica). However, based on previous known lengths of adult males (>4.2 m), it is likely that results here also represent adult males (N = 22 Tenerife, N = 3 Terceira, N = 0 Dominica). The locations of the sampled whales were 55 from Tenerife (6 calves, 18 juveniles, and 31 adults), 11 from Terceira (2 calves, 6 juveniles, and 3 adults), and 11 from Dominica (1 calf, 7 juveniles, and 3 adults). The seasons in which whales were sampled were winter (N = 8 Tenerife), spring (N = 40 Tenerife, N = 11 Dominica), and summer (N = 7 Tenerife, N = 11 Terceira). Dorsal (width) and dorso-ventral (height) measurements were obtained for eight whales (four calves, three juveniles, and one adult), which were used to calculate the HW ratio along the body (BL).

Table 2. Pilot whale lengths (m), volumes (m^3), and conditions of individuals sampled off Tenerife, Terceira, and Dominica. Values are means [min, max].

Reproductive Class	n	Body Length (m) Mean [min,max]	Body Volume (m^3) Mean [min,max]	Body Condition (%) Mean [min,max]
Calves	9	2.37 [2.09–2.48]	0.23 [0.15–0.32]	1.48 [−14.11–29.28]
Juveniles	31	2.90 [2.55–3.20]	0.39 [0.25–0.64]	0.93 [−34.75–52.43]
Adults	37	3.72 [3.20–4.57]	0.72 [0.46–1.13]	1.40 [−17.61–30.46]
Total	77	2.99 [2.09–4.57]	0.44 [0.15–1.13]	0.87 [−34.75–52.43]

3.2. Body Shape and Allometrics of Short-Finned Pilot Whales

The body morphometric data showed that the body shape was similar among reproductive classes, with the widest point of the animal being at approximately 30–35% BL (measured from the rostrum), where it was 15–17% of BL depending on the reproductive class (Figure 3). The widest section of the pilot whale was situated around the beginning of the dorsal fin. Anterior to this point, the width declined slowly towards the rostrum, with the head (<20%BL) width being approximately 12–16% of BL (Figure 2). Posterior of the widest point, the body width declined slowly to approximately 55%BL (at which point the relative width was ~14% of BL), after which it declined sharply in a linear fashion towards the fluke. Calves were relatively wider in body shape compared to juveniles and adults, especially across the anterior half of the body, including the head region (Figure 3). The allometric relationship between BL and the absolute rostrum–blowhole distance (LM: $F_{1,75}$ = 40.2, p < 0.001, R^2 = 0.349, Figure 4A) and the fluke width (LM: $F_{1,75}$ = 443.4, p < 0.001, R^2 = 0.855, Figure 4B) of pilot whales increased linearly with body length, whereas their relative measurements did not change with body length (Figure 4C,D).

The body shape of the pilot whales at transverse cross-sections was calculated along the body axis as HW ratios (Figure 5, Table S1). From the rostrum to the length of the body axis to approximately 65%BL, the cross-sectional body shape was quite constant, with the HW ratio ranging from 1.3–1.6 (Figure 3, Table S1). However, from around 65%BL to 85%BL, the peduncle and fluke stock region were considerably flattened in the lateral plane (with greater height contributions rather than width contributions; laterally compressed), with HW ratios increasing from 1.7 to 3.3 towards the beginning of the fluke (Figure 5, Table S1). The sample size was too small to investigate differences in HW ratios between reproductive classes.
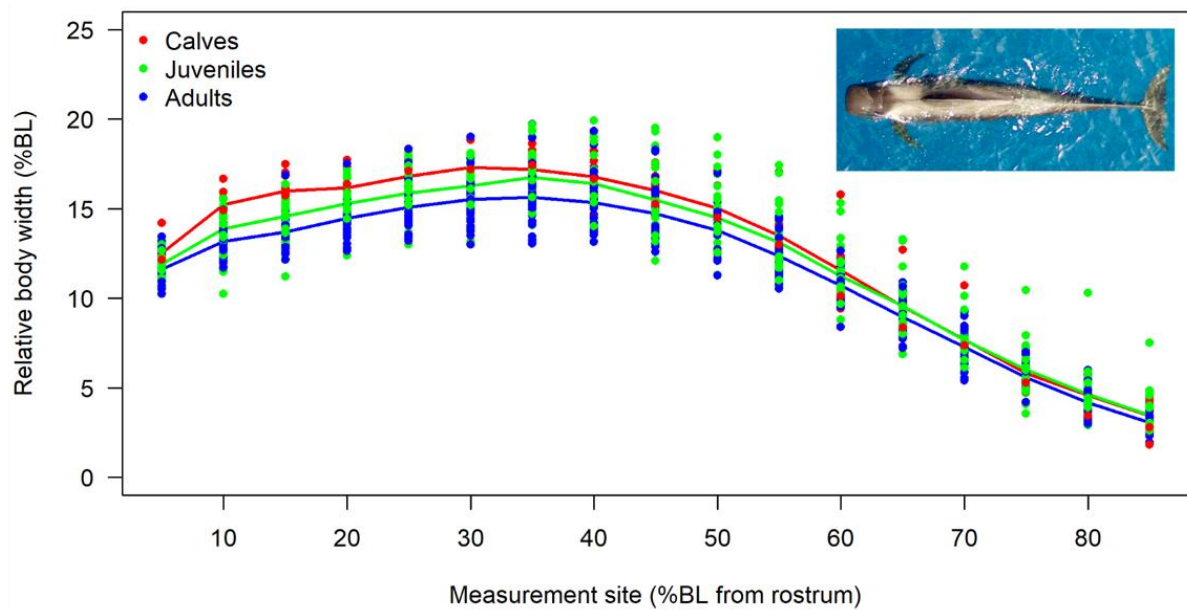
Figure 3. Mean relative body width (body width/body length, in %BL) of pilot whales at different measurement sites along the body axis (BL = body length; refer to Figure 2 for location of measurement sites). N = 77 (9 calves, 31 juveniles and 37 adults). Dots represent individual measurements at each site (77 measurements at each site), and the lines represent the mean for calves, juveniles, and adults (see colour legend). The body morphometric data showed that the body shape was similar among reproductive classes, with the widest point at approximately 30–35% BL.
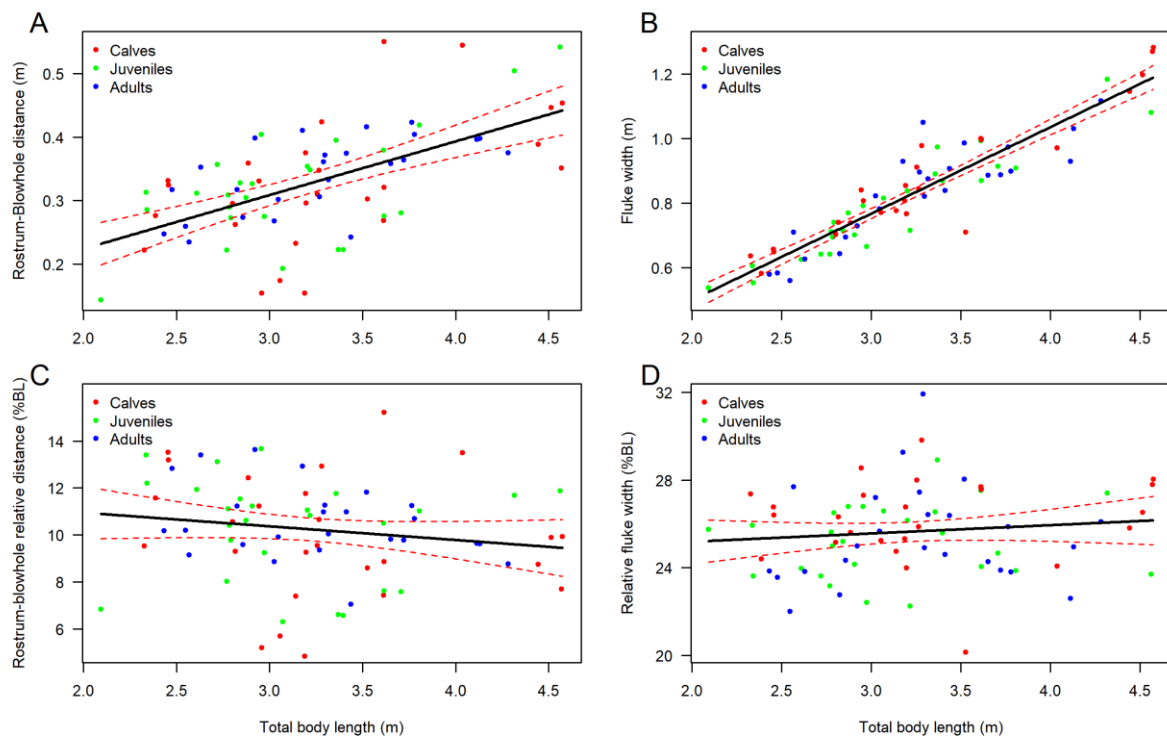

Figure 4. Allometric relationship between pilot whale body length (BL) and (**A**) rostrum−blowhole absolute distance (RBAbs = 0.055 + 0.085 × BL, R^2 = 0.349), (**B**) absolute fluke width (FWAbs = −0.036 + 0.268 × BL, R^2 = 0.855), (**C**) rostrum−blowhole relative distance, and (**D**) relative fluke width. N = 77 (9 calves, 31 juveniles, and 37 adults). Colours indicate the reproductive classes (see keys). The solid black lines represent the fitted value of the linear models. The dashed red lines indicate the 95% confidence intervals.
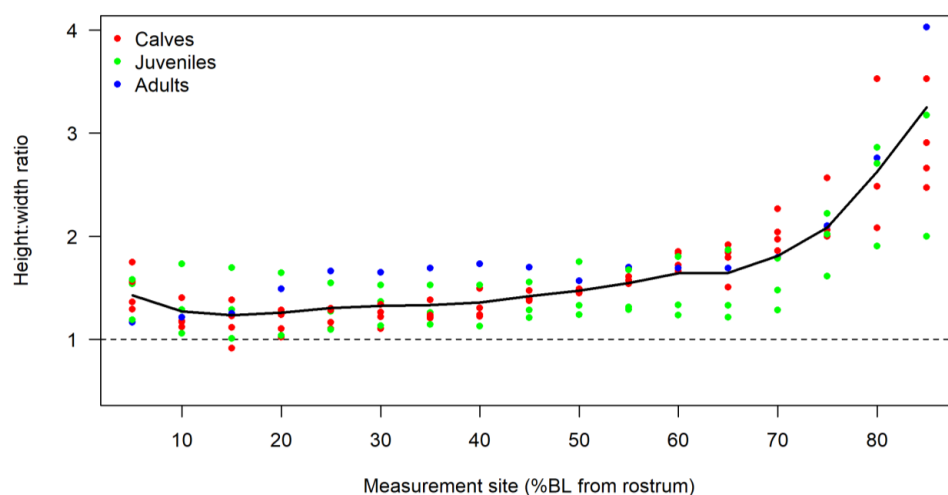
Figure 5. Body shape of pilot whales measured as a height:width (HW) ratio across the axis of the body from 5 to 85%BL from the rostrum to the fluke stock (see Figure 2 for location of measurement sites). N = 4 calves, 3 juveniles, and 1 adult. The solid black line represents the average HW ratio of measured whales. The dashed black line indicates an HW ratio of 1:1, equivalent to a circular cross-sectional body shape when cut in the transverse plane. Values above the line can be interpreted as the whale being taller than it is wide, and if the values went below the line, it would show that the whale is wider than it is taller.

3.3. Body Condition of Short-Finned Pilot Whales

The estimated body volume of pilot whales ranged between 0.15 and 0.32 m^3 (mean = 0.23 m^3, SD = 0.046) for calves, 0.25 and 0.64 m^3 (mean = 0.39 m^3, SD = 0.090) for juveniles, and 0.46 and 1.13 m^3 (mean = 0.72 m^3, SD = 0.205) for adults (Figure 5A, Table 2). The linear relationship between body volume (BV) and body length (BL) on the log-log scale was (LM: $F_{1,75}$ = 883.0, p < 0.001, Figure 6):

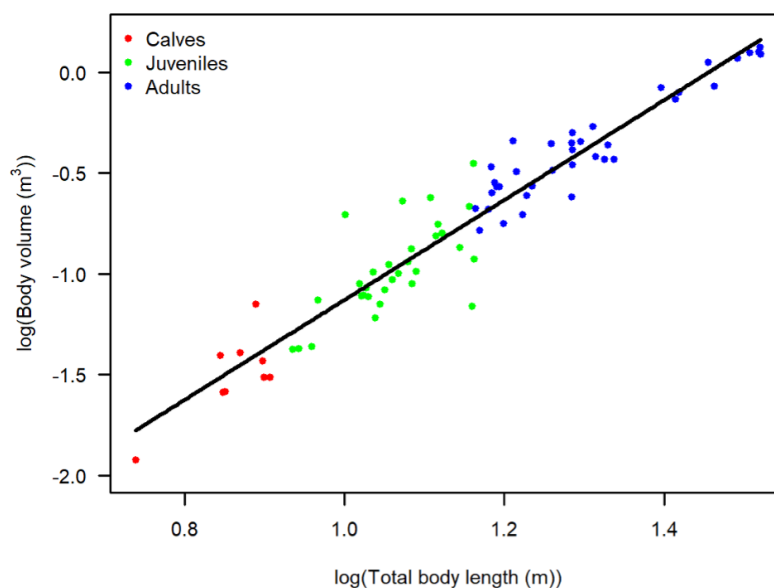$$\log(BV_{exp,i}) = -3.611 + 2.481 \times \log(BL_i) \tag{5}$$

Figure 6. The log - log relationship between body volume and body length for different reproductive age classes (see colour key). The solid black line represents the back-transformed fitted values of the linear model: log(BV) = −3.611 + 2.481 × log(BL), R^2 = 0.922. N = 77 (9 calves, 31 juveniles, and 37 adults).

The model explained 92.2% (R^2) of the variance in the body volume data. The resulting body condition of the whales ranged from −34.8 to +52.4% (mean = 0.0087, SD = 0.137). There was no difference in body condition between reproductive classes (LM: $F_{2,74}$ = 0.155, p = 0.856) or locations (LM: $F_{2,74}$ = 0.188, p = 0.829).

4. Discussion

We measured the body shape, allometrics, and body condition of short-finned pilot whales. To do this, we used UAV aerial photogrammetry to characterise the body condition across different reproductive classes from three different locations within the North Atlantic (Tenerife, Terceira, and Dominica). We found no difference in body condition among reproductive classes or locations.

4.1. Body Shape and Allometrics of Pilot Whales

Total length, measured from the tip of the rostrum to the tail notch [56], is a standardized parameter used in cetacean life history studies [57,58]. The total length of pilot whale was, on average, 2.37 m (SD = 0.11) in calves, 2.90 m (SD = 0.18) in juveniles, and 3.72 m (SD = 0.44) in adults. These results are comparable to the total length of newly (fresh) stranded short-finned pilot whales off the east and western North Atlantic Ocean, where the combined average length was 1.79 m (SD = 0.40, N = 14) for calves, 2.81 m (SD = 0.09, N = 103) for juveniles and 3.77 (SD = 0.15, N = 58) for adults [41,42,59] (Table 3). The average length of calves in our study was larger compared with the length of stranded calves in the North Atlantic. In some toothed whale species, such as common bottlenose dolphins, variation in calf length and subsequent first-year survival can be related to maternal investment, body mass, and condition (Cockcroft & Ross, 1990; Reed & Plante, 1997). Across the North Atlantic, short-finned pilot whales genetically sampled within the Caribbean (the Antilles and Florida), the east coast of the USA (Carolina), and Spain (the Canaries) constitute a single genetic morphotype [38]. These locations fall within the North Atlantic Gyre, an oblique oceanic current with thermohaline circulation, that bathes in a region between the Azores and the Cape Verde Islands in the east and the Antilles and Canada in the west [60]. Similar thermohaline conditions are found within the gyre, dominated by the Gulf Stream current in the west, bringing warm water from the Caribbean to the western coastlines of Europe and Africa [61]. This, together with the absence of geographic boundaries within the region may have contributed to the existence of a single short-finned pilot whale morphotype in the North Atlantic [38], as our morphometric data supports. Nonetheless, the collection of a larger sample size may be required in order to further explore potential differences in life-history parameters and morphology of known-age animals across areas.

Table 3. Length of pilot whales across different reproductive classes in the North Atlantic Ocean (free-ranging and stranded) and in captivity. Values represent mean (meters) with standard deviation in square brackets.

	North Atlantic (This Study)	Florida and South Carolina [41] *	North Carolina [42] **	Galicia (Eastern North Atlantic) [59] *	Captivity [62]
Calves	2.37 (0.11) N = 9	2.15 (0.12) N = 9	1.88 (0.27) N = 4	1.35 N = 1	NA
Juveniles	2.90 (0.18) N = 31	2.91 (0.24) N = 92	2.81 (0.28) N = 6	2.73 (0.42) N= 5	NA
Adults	3.72 (0.44) N = 37	3.80 (0.48) N = 35	3.60 (0.16) N = 17	3.91 (0.33) N = 6	3.85 (0.38) N = 5

* mass stranding, many measured alive; ** mass stranding, measured within 24 h from post-mortem. To note: Same classification of reproductive classes was applied across studies. Total length was measured from rostrum to tail notch [56].

Cetaceans have highly streamlined body shapes, as their lifestyle and foraging habits involve prolonged periods of swimming [35,63]. Pilot whales were elliptical in their cross-sectional shape and were more streamlined in the peduncle and tail stock region. The tail stock was laterally compressed, which is highly adapted for this deep-diving species [45,55]. Although there were limited measurements to compare among reproductive classes, calves appeared to not be as streamlined as juveniles and adults based on Figure 5. Streamlining and buoyancy capacities needed for efficient hydrodynamic locomotion are believed to develop later in the juvenile years [28,64–66]. It has been observed that calves acquire a more streamlined body shape with length, which is also reported in southern right whales (*Eubalaena australis*) [67] and bottlenose dolphins (*T. truncatus*) [68]. The body shape of pilot whales was widest at 30–35% of the BL, roughly corresponding to the anterior dorsal fin area. Our results are comparable to those found in short-finned pilot whales in captivity, where body width was the widest when measured at the anterior dorsal fin site, compared to anterior pectoral and posterior dorsal fin sites [62]. Similarly, the mean surface area between anterior and posterior dorsal fin sites, when estimated as a truncated cone model, was higher compared to other sections of the body [28]. Similarly, Antarctic minke whales (*Balaenoptera bonaerensis*) and blue whales (*Balaenoptera musculus*) exhibit the widest points around 30–40% of the BL, respectively [69]. On the other hand, the cross-sectional body shape of the anterior half of the body in humpback whales and gray whales is close to circular (HW ratio≈1) with the widest point measured at approximately 40–45% of the BL [10,26]. Further studies including known sex and reproductive classes of individuals can be conducted to further explore differences in body shape and how shape relates to streamlining and buoyancy capacity within cetaceans.

For toothed whales that are sexually dimorphic in body size, sexual size dimorphism scales allometrically with body size [70]. As reported in other sexually dimorphic toothed whale species [71,72], our study found allometric growth in pilot whales. The allometric relationship between body length and rostrum to blowhole absolute distance, and fluke width, increased linearly for all three reproductive classes and showed no inflexions indicating that the growth of the forehead and fluke of this species is widest in larger individuals. These results differ from those in both male and female common dolphins (*Delphinus delphis*) [70], where these measurements present isometric growth, apart from the relationship between body length and rostrum to the blowhole in females [73]. Similarly, Common and Indo-Pacific bottlenose dolphins (*Tursiops aduncus*) exhibit similar growth curves for males and females [57,74], leading to moderate, less-pronounced sexual dimorphism in this species. Pilot whale ontogenetic allometries may result in disproportionally larger foreheads and tails in adult pilot whales [51], leading to a marked male-biased sexual dimorphism in this species.

4.2. Body Condition of Pilot Whales

Changes in body mass in non-fasting small-bodied cetaceans such as pilot whales correlate well with blubber changes at specific body sections (i.e., where blubber is metabolically active) allowing estimation of the body condition from body length and width measurements [62,75]. Furthermore, the body condition can also be expressed more accurately by constructing volumetric models for the species, including body height (from images of rolling free-ranging whales, or from 3D models) or girth measurements (in the case of dead specimens), a technique initially developed for baleen whales [17,25] and later applied to odontocete species, such as harbour porpoises [76], sperm whales [27], and pilot whales [28]. Using the information on the cross-sectional body shape of the individuals provides a more accurate representation of the true body shape and volume to estimate the body condition of the animals. Here, we used body measurements from aerial photographs to calculate the relative body width and shape of the whales at transverse cross-sections (Figure 2C). Despite the resulting wide variation in the pilot whale body condition found in this study (range −34.8 to +52.4%), no significant differences were found across locations or reproductive classes.

Adaptations to habitat conditions, i.e., variations in lipid storage to adjust body density to feed on specific prey types and distributions, can influence body conditions in marine mammals [77,78]. Foraging hot spots for short-finned pilot whales along the US coast (including Hawaii) and Macaronesia have been associated with steep bathymetric gradients and the midwater slope [35,79–81]. This likely led to the development of a comparable foraging strategy [45,79] for this species across the North Atlantic. This further supports the results, whereby there is a similar body condition in pilot whales across sampled locations. A better body condition (e.g., low surface-area-to-volume ratio, resulting from a thick blubber layer) not only acts as an energy reserve but can also provide thermal insulation [82]. Seasonal changes in the body condition of free-ranging cetaceans have been documented in fin whales (*Balaenoptera physalus*) [82], humpback whales [26], gray whales [83], and long-finned pilot whales [84], but they have not been tested in short-finned pilot whales. Seasonality was suggested in the short-finned pilot whale in captivity, although this may be due to water temperature differences in pool conditions [62]. Long-finned pilot whales are primarily a temperate species compared to short-finned pilot whales and have a fattening period over winter and spring when water temperatures are cooler, compared to summer when water temperatures are warmer (overall range across seasons 13–25 °C) [62,84]. Seasonal changes in body condition could not be tested in this study due to sample size. Pilot whales in Tenerife were sampled in winter (N = 8), spring (N = 40) and summer (N = 7) seasons, whereas off Terceira and Dominica, pilot whales were sampled in spring and summer. However, small variations in sea surface temperature in the tropical and subtropical North Atlantic, e.g., average annual water temperature difference of 5 °C in the Canaries (overall range across seasons 18–23 °C) [85], may not transpire into significant changes in the body condition of short-finned pilot whales. Future studies could examine any seasonality within short-finned pilot whales' body condition.

A limitation of this study was that the sex of individuals was unknown. Future studies could incorporate data to determine the sex, especially as short-finned pilot whales exhibit striking sexual dimorphism in adult body size [31,86]. Sexual dimorphism in body size is also observed in other odontocetes, including sperm whales [87], killer whales [68], and long-finned pilot whales [35], where males are larger than females. In short-finned pilot whales, adult males are, on average, 24% longer than females (Table 1) [31,86], and preferential associations and segregation between adult males and female–calf pairs occur in this species [88]. Sampling of single groups generally found at particular locations may therefore not be representative of body length variation within a given population. Further sampling of short-finned pilot whale groups in other locations including a range of reproductive and sex classes will improve the interpretation of results to understand the contribution of sexual dimorphism between the sexes. Furthermore, repeated photogrammetric measures on the same individuals over time, using lateral photographs of their dorsal fin or genetic sampling to identify and distinguish between conspecifics, can provide invaluable information on body condition (e.g., [12]). For example, the body condition of females is particularly important, as a reduction in body condition in reproductive females may influence the pregnancy rate [14], foetus development [16], and offspring survival [20]. Females can be identified from aerial videos or photographs based on the presence of mother–calf pair associations, or when animals are inverted, and photographs of the genital area are clearly inspected and matched to the individual. Even though pilot whales are sexually dimorphic, the sexes cannot be visually determined easily in the field, for example, based on the size of their dorsal fins [89]. Furthermore, UAV photogrammetry combined with life history information can help to identify and routinely monitor pregnancy rates and reproductive success, which are critical components to assess both the health of the population and individual fitness [29].

4.3. Future Conservation Efforts

Differences in exposure to anthropogenic factors can drive potential differences in body conditions between study areas [11]. Deep-diving short-finned pilot whales can be

found relatively close to shore in oceanic islands and in other steep-slope areas [48,79–81], where they are vulnerable to anthropogenic factors such as vessel noise [46,47,90] and ship strikes [91,92]. Vessel noise is a primary driver of behavioural disturbance in cetaceans targeted by whale-watching activities [93]. In the presence of whale-watching vessels, resident short-finned pilot whales show a decrease in resting and nursing [47]. Such disruptions in the activity budget could lead to long-term bioenergetic effects, such as reduced body condition/health [94] and habitat displacement [95], amongst others, leading to a reduction in survival and fecundity, and ultimately (if enough individuals are affected), a decrease in population size [96]. To mitigate this threat, long-term monitoring of the body condition of free-ranging short-finned pilot whales with non-invasive emerging techniques, such as aerial photogrammetry, combined with sampling for sex and hormone-based stress level assessment, will allow new quantitative models to be developed that will lead to a better understanding of the vulnerability of pilot whale populations to anthropogenic stressors.

References

1. Wilder, S.M.; Raubenheimer, D.; Simpson, S.J. Moving beyond body condition indices as an estimate of fitness in ecological and evolutionary studies. *Funct. Ecol.* **2016**, *30*, 108–115. [CrossRef]
2. Jakob, E.M.; Marshall, S.D.; Uetz, G.W. Estimating Fitness: A Comparison of Body Condition Indices. *Oikos* **1996**, *77*, 61–67. [CrossRef]
3. Gaillard, J.-M.; Festa-Bianchet, M.; Delorme, D.; Jorgenson, J. Body mass and individual fitness in female ungulates: Bigger is not always better. *Proc. R. Soc. B Boil. Sci.* **2000**, *267*, 471–477. [CrossRef] [PubMed]

4. Toïgo, C.; Gaillard, J.-M.; Van Laere, G.; Hewison, M.; Morellet, N. How does environmental variation influence body mass, body size, and body condition? Roe deer as a case study. *Ecography* **2006**, *29*, 301–308. [CrossRef]

5. Tartu, S.; Bourgeon, S.; Aars, J.; Andersen, M.; Polder, A.; Thiemann, G.W.; Welker, J.M.; Routti, H. Sea ice-associated decline in body condition leads to increased concentrations of lipophilic pollutants in polar bears (*Ursus maritimus*) from Svalbard, Norway. *Sci. Total Environ.* **2017**, *576*, 409–419. [CrossRef]

6. Pettis, H.; Rolland, R.; Hamilton, P.; Knowlton, A.; Burgess, E.; Kraus, S. Body condition changes from natural factors and fishing gear entanglements in North Atlantic right whales Eubalaena glacialis. *Endanger. Species Res.* **2016**, *32*, 237–249. [CrossRef]

7. Ijsseldijk, L.L.; Hessing, S.; Mairo, A.; Doeschate, M.T.I.T.; Treep, J.; Broek, J.V.D.; Keijl, G.O.; Siebert, U.; Heesterbeek, H.; Gröne, A.; et al. Nutritional status and prey energy density govern reproductive success in a small cetacean. *Sci. Rep.* **2021**, *11*, 19201. [CrossRef]

8. Lockyer, C.; Waters, T. Weights and anatomical measurements of Northeastern Atlantic Fin (*Balaenoptera physalus*, linnaeus) and Sei (*B. borealis*, lesson) whales. *Mar. Mammal Sci.* **1986**, *2*, 169–185. [CrossRef]

9. Braithwaite, J.E.; Meeuwig, J.J.; Letessier, T.B.; Jenner, K.C.S.; Brierley, A.S. From sea ice to blubber: Linking whale condition to krill abundance using historical whaling records. *Polar Biol.* **2015**, *38*, 1195–1202. [CrossRef]

10. Christiansen, F.; Rodríguez-González, F.; Martínez-Aguilar, S.; Urbán, J.; Swartz, S.; Warick, H.; Vivier, F.; Bejder, L. Poor body condition associated with an unusual mortality event in gray whales. *Mar. Ecol. Prog. Ser.* **2021**, *658*, 237–252. [CrossRef]

11. Christiansen, F.; Dawson, S.; Durban, J.; Fearnbach, H.; Miller, C.; Bejder, L.; Uhart, M.; Sironi, M.; Corkeron, P.; Rayment, W.; et al. Population comparison of right whale body condition reveals poor state of the North Atlantic right whale. *Mar. Ecol. Prog. Ser.* **2020**, *640*, 1–16. [CrossRef]

12. Currie, J.J.; van Aswegen, M.; Stack, S.H.; West, K.L.; Vivier, F.; Bejder, L. Rapid weight loss in free ranging pygmy killer whales (*Feresa attenuata*) and the implications for anthropogenic disturbance of odontocetes. *Sci. Rep.* **2021**, *11*, 8181. [CrossRef] [PubMed]

13. Kershaw, J.L.; Ramp, C.A.; Sears, R.; Plourde, S.; Brosset, P.; Miller, P.J.; Hall, A.J. Declining reproductive success in the Gulf of St. Lawrence's humpback whales (*Megaptera novaeangliae*) reflects ecosystem shifts on their feeding grounds. *Glob. Chang. Biol.* **2021**, *27*, 1027–1041. [CrossRef] [PubMed]

14. Williams, R.; Víkingsson, G.; Gislason, A.; Lockyer, C.; New, L.; Thomas, L.; Hammond, P.S. Evidence for density-dependent changes in body condition and pregnancy rate of North Atlantic fin whales over four decades of varying environmental conditions. *ICES J. Mar. Sci.* **2013**, *70*, 1273–1280. [CrossRef]

15. Lockyer, C. All creatures great and smaller: A study in cetacean life history energetics. *J. Mar. Biol. Assoc. UK* **2007**, *87*, 1035–1045. [CrossRef]

16. Christiansen, F.; Vikingsson, G.A.; Rasmussen, M.H.; Lusseau, D. Female body condition affects foetal growth in a capital breeding mysticete. *Funct. Ecol.* **2014**, *28*, 579–588. [CrossRef]

17. Christiansen, F.; Vivier, F.; Charlton, C.; Ward, R.; Amerson, A.; Burnell, S.; Bejder, L. Maternal body size and condition determine calf growth rates in southern right whales. *Mar. Ecol. Prog. Ser.* **2018**, *592*, 267–281. [CrossRef]

18. Castrillon, J.; Bengtson Nash, S. Evaluating cetacean body condition; a review of traditional approaches and new developments. *Ecol. Evol.* **2020**, *10*, 6144–6162. [CrossRef]

19. Durban, J.W.; Moore, M.J.; Chiang, G.; Hickmott, L.S.; Bocconcelli, A.; Howes, G.; Bahamonde, P.A.; Perryman, W.L.; Leroi, D.J. Photogrammetry of blue whales with an unmanned hexacopter. *Mar. Mammal Sci.* **2016**, *32*, 1510–1515. [CrossRef]

20. Christiansen, F.; Dujon, A.M.; Sprogis, K.R.; Arnould, J.P.Y.; Bejder, L. Noninvasive unmanned aerial vehicle provides estimates of the energetic cost of reproduction in humpback whales. *Ecosphere* **2016**, *7*, e01468. [CrossRef]

21. Fearnbach, H.; Durban, J.; Ellifrit, D.; Balcomb, K. Using aerial photogrammetry to detect changes in body condition of endangered southern resident killer whales. *Endanger. Species Res.* **2018**, *35*, 175–180. [CrossRef]

22. Buckland, S.T.; Garner, G.W.; Amstrup, S.C.; Laake, J.L.; Manly, B.F.J.; McDonald, L.L.; Robertson, D.G. *Marine Mammal Survey and Assessment Methods*; Balkema, A.A., Ed.; CRC Press: Rotterdam, The Netherlands; Brookfield, WI, USA, 1999; p. 177.

23. Buckland, S.T.; Anderson, D.R.; Burnham, K.P.; Laake, J.L. *Distance Sampling*; Hall, C.A., Ed.; John Wiley & Sons, Ltd.: London, UK, 1993.

24. Christie, A.I.; Colefax, A.P.; Cagnazzi, D. Feasibility of Using Small UAVs to Derive Morphometric Measurements of Australian Snubfin (*Orcaella heinsohni*) and Humpback (*Sousa sahulensis*) Dolphins. *Remote Sens.* **2022**, *14*, 21. [CrossRef]

25. Christiansen, F.; Sironi, M.; Moore, M.J.; Di Martino, M.; Ricciardi, M.; Warick, H.A.; Irschick, D.J.; Gutierrez, R.; Uhart, M.M. Estimating body mass of free-living whales using aerial photogrammetry and 3D volumetrics. *Methods Ecol. Evol.* **2019**, *10*, 2034–2044. [CrossRef]

26. Christiansen, F.; Sprogis, K.R.; Groß, J.; Castrillon, J.; Warick, H.A.; Leunissen, E.; Nash, S.B. Variation in outer blubber lipid concentration does not reflect morphological body condition in humpback whales. *J. Exp. Biol.* **2020**, *223*, jeb213769. [CrossRef] [PubMed]

27. Glarou, M.; Gero, S.; Frantzis, A.; Brotons, J.M.; Vivier, F.; Alexiadou, P.; Cerdà, M.; Pirotta, E.; Christiansen, F. Estimating body mass of sperm whales from aerial photographs. *Mar. Mammal Sci.* **2022**, 1–23. [CrossRef]

28. Adamczak, S.K.; Pabst, A.; McLellan, W.A.; Thorne, L.H. Using 3D Models to Improve Estimates of Marine Mammal Size and External Morphology. *Front. Mar. Sci.* **2019**, *6*, 334. [CrossRef]

29. Cheney, B.J.; Dale, J.; Thompson, P.M.; Quick, N.J. Spy in the sky: A method to identify pregnant small cetaceans. *Remote Sens. Ecol. Conserv.* **2022**, *8*, 492–505. [CrossRef]

30. Stewart, J.D.; Durban, J.W.; Fearnbach, H.; Barrett-Lennard, L.G.; Casler, P.K.; Ward, E.J.; Dapp, D.R. Survival of the fattest: Linking body condition to prey availability and survivorship of killer whales. *Ecosphere* **2021**, *12*, e03660. [CrossRef]

31. Kasuya, T.; Matsui, S. Age determination and growth of the short finned pilot whale off the pacific coast of Japan. *Sci. Rep. Whales Res. Inst.* **1984**, *35*, 57–91.

32. Heimlich-Boran, J.R. *Social Organisation of the Short-Finned Pilot Whale (Globicephala macrorhynchus) with Special Reference to the Comparative Social Ecology of Delphinids*; University of Cambridge: Cambridge, UK, 1993.

33. Kasuya, T.; Tai, S. Life history of short finned pilot whale stocks off Japan and a description of the fishery. In *Biology of Northern Hemisphere Pilot Whales*; Donova, G., Lockyer, C., MArtin, A., Eds.; IWC: Cambridge, UK, 1993; p. 479.

34. Alves, F.; Dinis, A.; Nicolau, C.; Ribeiro, C.; Kaufmann, M.; Fortuna, C.; Freitas, L. Survival and abundance of short-finned pilot whales in the archipelago of Madeira, NE Atlantic. *Mar. Mammal Sci.* **2015**, *in press*. [CrossRef]

35. Würsig, B.; Thewissen, J.G.M.; Kovacs, K. *Encyclopedia of Marine Mammals*, 3rd ed.; Academic Press: London, UK, 2018.

36. Téllez, R.; Mignucci-Giannoni, A.A.; Caballero, S. Initial description of short-finned pilot whale (*Globicephala macrorhynchus*) genetic diversity from the Caribbean. *Biochem. Syst. Ecol.* **2014**, *56*, 196–201. [CrossRef]

37. Caldwell, D.K.; Erdman, D.S. The Pilot Whale in the West Indies. *J. Mammal.* **1963**, *44*, 113–115. [CrossRef]

38. Van Cise, A.M.; Baird, R.W.; Baker, C.S.; Cerchio, S.; Claridge, D.; Fielding, R.; Hancock-Hanser, B.; Marrero, J.; Martien, K.K.; Mignucci-Giannoni, A.A.; et al. Oceanographic barriers, divergence, and admixture: Phylogeography and taxonomy of two putative subspecies of short-finned pilot whale. *Mol. Ecol.* **2019**, *28*, 2886–2902. [CrossRef] [PubMed]

39. Kasuya, T.; Mayashita, T.; Kasamatsu, F. Segregation of two forms of short finned pilot whales off the Pacific coast of Japan. *Sci. Rep. Whales Res. Inst.* **1988**, *39*, 77–90.

40. Oremus, M.; Gales, R.; Dalebout, M.L.; Funahashi, N.; Endo, T.; Kage, T.; Steel, D.; Baker, S.C. Worldwide mitochondrial DNA diversity and phylogeography of pilot whales (*Globicephala* spp.). *Biol. J. Linn. Soc.* **2009**, *98*, 729–744. [CrossRef]

41. Irvine, A.B.; Scott, M.D.; Wells, R.S.; Mead, J.G. Stranding of the pilot whale, *Globicephala macrorhynchus*, in Florida and South Carolina. *Fish. Bull.* **1979**, *77*, 511–513.

42. Hohn, A.A.; Rotstein, D.S.; Harms, C.A.; Southall, B.L. Report on Marine Mammal Unusual Mortality Event UMESE0501Sp: Multispecies Mass Stranding of Pilot Whales (*Globicephala macrorhynchus*), Minke Whale (*Balaenoptera acutorostrata*) and Dwarf Sperm Whales (*Kogia sima*) in North Carolina on 15–16 January 2005. Noaa Technical Memorandum Nmfs-Sefsc-537. 2006. Available online: https://aquadocs.org/handle/1834/19915 (accessed on 23 June 2022).

43. Kasuya, T.; Marsh, H. Life history and reproductive biology of the short-finned pilot whale, *Globicephala macrorhynchus*, off the Pacific coast of Japan. *Rep. Int. Whal. Commn. Spec. Issue* **1984**, *6*, 259–310.

44. Ellis, S.; Franks, D.W.; Nattrass, S.; Currie, T.E.; Cant, M.A.; Giles, D.; Balcomb, K.C.; Croft, D.P. Analyses of ovarian activity reveal repeated evolution of post-reproductive lifespans in toothed whales. *Sci. Rep.* **2018**, *8*, 12833. [CrossRef]

45. Soto, N.A.; Johnson, M.P.; Madsen, P.T.; Díaz, F.; Domínguez, I.; Brito, A.; Tyack, P. Cheetahs of the deep sea: Deep foraging sprints in short finned pilot whales off Tenerife (Canary Islands). *J. Anim. Ecol.* **2008**, *77*, 936–947. [CrossRef]

46. Jensen, F.H.; Bejder, L.; Wahlberg, M.; de Soto, N.A.; Johnson, M.; Madsen, P. Vessel noise effects on delphinid communication. *Mar. Ecol. Prog. Ser.* **2009**, *395*, 161–175. [CrossRef]

47. Arranz, P.; Glarou, M.; Sprogis, K.R. Decreased resting and nursing in short-finned pilot whales when exposed to louder petrol engine noise of a hybrid whale-watch vessel. *Sci. Rep.* **2021**, *11*, 21195. [CrossRef] [PubMed]

48. Servidio, A.; Pérez-Gil, E.; Pérez-Gil, M.; Cañadas, A.; Hammond, P.S.; Martín, V. Site fidelity and movement patterns of short-finned pilot whales within the Canary Islands: Evidence for resident and transient populations. *Aquat. Conserv. Mar. Freshw. Ecosyst.* **2019**, *29* (Suppl. S1), 227–241. [CrossRef]

49. Silva, M.A.; Prieto, R.; Cascão, I.; Seabra, M.; Machete, M.; Baumgartner, M.F.; Santos, R.S. Spatial and temporal distribution of cetaceans in the mid-Atlantic waters around the Azores. *Mar. Biol. Res.* **2014**, *10*, 123–137. [CrossRef]

50. Boisseau, O.; Leaper, R.; Moscrop, A. *Observations of Small Cetaceans in the Eastern Caribbean*; International Whaling Commission Scientific Committee Paper SC/58/SM24; International Whaling Commission Scientific Committee: Munich, Germany, 2006.

51. Jefferson, T.; Webber, M.; Pitman, R.L. *Marine Mammals of the World: A Comprehensive Guide to Their Identification. Marine Mammals of the World: A Comprehensive Guide to Their Identification*; Elsevier: Amsterdam, The Netherland, 2008.

52. Servidio, A. Distribution, Social Structure and Habitat Use of Short-Finned Pilot Whale, *Globicephala macrorhynchus*, in the Canary Islands. Ph.D. Thesis, University of St Andrews, St Andrews, UK, 2014.

53. Puig-Lozano, R.; Fernández, A.; Saavedra, P.; Tejedor, M.; Sierra, E.; De La Fuente, J.; Xuriach, A.; Díaz-Delgado, J.; Rivero, M.A.; Andrada, M.; et al. Retrospective Study of Traumatic Intra-Interspecific Interactions in Stranded Cetaceans, Canary Islands. *Front. Vet. Sci.* **2020**, *7*, 107. [CrossRef]

54. Prieto, R.; Fernandes, M. Revision of the occurrence of the long-finned pilot whale *Globicephala melas* (Traill, 1809), in the Azores. *Arquipel.-Life Mar. Sci.* **2007**, *24*, 65–69.

55. Arkowitz, R.; Rommel, S. Force and bending moment of the caudal muscles in the shortfin pilot whale. *Mar. Mammal Sci.* **1985**, *1*, 203–209. [CrossRef]

56. Norris, K.S. Standardized methods for measuring and recording data on smaller cetaceans. *J. Mammal.* **1961**, *42*, 471–476. [CrossRef]

57. Cheney, B.; Wells, R.S.; Barton, T.R.; Thompson, P.M. Laser photogrammetry reveals variation in growth and early survival in free-ranging bottlenose dolphins. *Anim. Conserv.* **2018**, *21*, 252–261. [CrossRef]

58. Dawson, S.M.; Bowma, M.H.; Leunissen, E.; Sirguey, P. Inexpensive Aerial Photogrammetry for Studies of Whales and Large Marine Animals. *Front. Mar. Sci.* **2017**, *4*, 366. [CrossRef]

59. Gonzalez, A.; Lopez, A. First recorded mass stranding of short finned pilot whales (*Globicephala macrorhynchus*) in the northeastern Atlantic. *Mar. Mammal Sci.* **2000**, *16*, 640–646. [CrossRef]

60. Alves, M.; Gaillard, F.; Sparrow, M.; Knoll, M.; Giraud, S. Circulation patterns and transport of the Azores Front-Current system. *Deep.-Sea Res. II* **2002**, *19*, 3983–4002. [CrossRef]

61. Minobe, S.; Kuwano-Yoshida, A.; Komori, N.; Xie, S.-P.; Small, R.J. Influence of the Gulf Stream on the troposphere. *Nature* **2008**, *452*, 206–209. [CrossRef] [PubMed]

62. Noren, S.; Schwarz, L.; Chase, K.; Aldrich, K.; Oss, K.M.-V.; Leger, J.S. Validation of the photogrammetric method to assess body condition of an odontocete, the shortfinned pilot whale *Globicephala macrorhynchus*. *Mar. Ecol. Prog. Ser.* **2019**, *620*, 185–200. [CrossRef]

63. Fish, F.E.; Howle, L.E.; Murray, M.M. Hydrodynamic flow control in marine mammals. *Integr. Comp. Biol.* **2008**, *48*, 788–800. [CrossRef] [PubMed]

64. Pabst, D.A. To bend a dolphin: Convergence of force transmission designs in cetaceans and scombrid fishes. *Am. Zool.* **2000**, *40*, 146–155. [CrossRef]

65. Mclellan, W.A.; Koopman, H.N.; Rommel, S.A.; Read, A.J.; Potter, C.W.; Nicolas, J.R.; Westgate, A.J.; Pabst, D.A. Ontogenetic allometry and body composition of harbour porpoises (*Phocoena phocoena*, L.) from the western North Atlantic. *J. Zool.* **2002**, *257*, 457–471. [CrossRef]

66. Tønnesen, P.; Gero, S.; Ladegaard, M.; Johnson, M.; Madsen, P.T. First-year sperm whale calves echolocate and perform long, deep dives. *Behav. Ecol. Sociobiol.* **2018**, *72*, 165. [CrossRef]

67. Marón, C.F.; Lábaque, M.C.; Beltramio, L.; Di Martino, M.; Alzugaray, L.; Ricciardi, M.; Ajó, A.A.F.; Adler, F.R.; Seger, J.; Sironi, M.; et al. Patterns of blubber fat deposition and evaluation of body condition in growing southern right whale calves (*Eubalaena australis*). *Mar. Mammal Sci.* **2021**, *37*, 1309–1329. [CrossRef]

68. Adamczak, S.K.; Holser, R.R.; Costa, D.P.; McCabe, E.J.B.; Wells, R.S. Body Composition of Common Bottlenose Dolphins in Sarasota Bay, Florida. *Front. Mar. Sci.* **2021**, *8*, 581. [CrossRef]

69. Bierlich, K.C.; Hewitt, J.; Bird, C.N.; Schick, R.S.; Friedlaender, A.; Torres, L.G.; Dale, J.; Goldbogen, J.; Read, A.J.; Calambokidis, J.; et al. Comparing Uncertainty Associated with 1-, 2-, and 3D Aerial Photogrammetry-Based Body Condition Measurements of Baleen Whales. *Front. Mar. Sci.* **2021**, *8*, 1729. [CrossRef]

70. Abouheif, E.; Fairbairn, D.J. A comparative analysis of allometry for sexual size dimorphism: Assessing Rensch's rule. *Am. Nat.* **1997**, *149*, 540–562. [CrossRef]

71. Clark, S.; Odell, D. Allometric Relationships and Sexual Dimorphism in Captive Killer Whales (*Orcinus orca*). *J. Mammal.* **1999**, *80*, 777. [CrossRef]

72. Dawson, S.M.; Chessum, C.J.; Hunt, P.J.; Slooten, E. An Inexpensive, Stereophotographic Technique to Measure Sperm Whales from Small Boats. *Rep. Int. Whal. Comm.* **1995**, *45*, 431–436.

73. Murphy, S.; Rogan, E. External morphology of the short-beaked common dolphin, Delphinus delphis: Growth, allometric relationships and sexual dimorphism. *Acta Zool.* **2006**, *87*, 315–329. [CrossRef]

74. van Aswegen, M.; Christiansen, F.; Symons, J.; Mann, J.; Nicholson, K.; Sprogis, K.; Bejder, L. Morphological differences between coastal bottlenose dolphin (*Tursiops aduncus*) populations identified using non-invasive stereo-laser photogrammetry. *Sci. Rep.* **2019**, *9*, 12235. [CrossRef]

75. Noren, S.R.; Schwarz, L.; Robeck, T.R. Topographic Variations in Mobilization of Blubber in Relation to Changes in Body Mass in Short-Finned Pilot Whales (*Globicephala macrorhynchus*). *Physiol. Biochem. Zool.* **2021**, *94*, 228–240. [CrossRef]

76. Irschick, D.J.; Martin, J.; Siebert, U.; Kristensen, J.H.; Madsen, P.T.; Christiansen, F. Creation of accurate 3D models of harbor porpoises (*Phocoena phocoena*) using 3D photogrammetry. *Mar. Mammal Sci.* **2021**, *37*, 482–491. [CrossRef]

77. Biuw, M.; McConnell, B.; Bradshaw, C.; Burton, H.; Fedak, M. Blubber and buoyancy: Monitoring the body condition of free-ranging seals using simple dive characteristics. *J. Exp. Biol.* **2003**, *206*, 3405–3423. [CrossRef]

78. Narazaki, T.; Isojunno, S.; Nowacek, D.P.; Swift, R.; Friedlaender, A.S.; Ramp, C.; Smout, S.; Aoki, K.; Deecke, V.B.; Sato, K.; et al. Body density of humpback whales (*Megaptera novaengliae*) in feeding aggregations estimated from hydrodynamic gliding performance. *PLoS ONE* **2018**, *13*, e0200287. [CrossRef]

79. Thorne, L.H.; Foley, H.J.; Baird, R.W.; Webster, D.L.; Swaim, Z.T.; Read, A.J. Movement and foraging behavior of short-finned pilot whales in the Mid-Atlantic Bight: Importance of bathymetric features and implications for management. *Mar. Ecol. Prog. Ser.* **2017**, *584*, 245–257. [CrossRef]

80. Abecassis, M.; Polovina, J.; Baird, R.; Copeland, A.; Drazen, J.; Domokos, R.; Oleson, E.; Jia, Y.; Schorr, G.S.; Webster, D.L.; et al. Characterizing a Foraging Hotspot for Short-Finned Pilot Whales and Blainville's Beaked Whales Located off the West Side of Hawai'i Island by Using Tagging and Oceanographic Data. *PLoS ONE* **2015**, *10*, e0142628. [CrossRef]

81. Fernandez, M.; Alves, F.; Ferreira, R.; Fischer, J.-C.; Thake, P.; Nunes, N.; Caldeira, R.; Dinis, A. Modeling Fine-Scale Cetaceans' Distributions in Oceanic Islands: Madeira Archipelago as a Case Study. *Front. Mar. Sci.* **2021**, *8*, 870. [CrossRef]

82. Víkingsson, G.A. Body condition of fin whales during summer off Iceland. In *Developments in Marine Biology*; Blix, A.S., Walløe, L., Ulltang, Ø., Eds.; Elsevier Science: New York, NY, USA, 1995; pp. 361–369.

83. Lemos, L.S.; Burnett, J.D.; Chandler, T.E.; Sumich, J.L.; Torres, L.G. Intra- and inter-annual variation in gray whale body condition on a foraging ground. *Ecosphere* **2020**, *11*, e03094.

84. Lockyer, C.H. Seasonal changes in body fat condition of northeast Atlantic pilot whales, and their biological significance. *Rep. Int. Whal. Comm. Spec. Issue* **1993**, *14*, 324–350.

85. Vélez-Belchí, P.; González-Carballo, M.; Pérez-Hernández, M.D.; Hernández-Guerra, A. *Open Ocean Temperature and Salinity Trends in the Canary Current Large Marine Ecosystem. Oceanographic and Biological Features in the Canary Current Large Marine Ecosystem*; Valdés, L., Déniz-Gonzalez, I., Eds.; IOC Technical Series; IOC-UNESCO: Paris, France, 2015; Volume 115.

86. Yonekura, M.; Matsui, S.; Kasuya, T. On the external characters of *Globicephala macrorhynchus* off Taiji, Pacific coast of Japan. *Sci. Rep. Whales Res. Inst.* **1980**, *32*, 67–95.

87. Cantor, M.; Gero, S.; Whitehead, H.; Rendell, L. *Sperm Whale: The Largest Toothed Creature on Earth, in Ethology and Behavioral Ecology of Odontocetes*; Springer: Berlin/Heidelberg, Germany, 2019; pp. 261–280.

88. Mahaffy, S.D.; Baird, R.W.; McSweeney, D.J.; Webster, D.L.; Schorr, G.S. High site fidelity, strong associations, and long-term bonds: Short-finned pilot whales off the island of Hawai'i. *Mar. Mammal Sci.* **2015**, *31*, 1427–1451. [CrossRef]

89. Augusto, J.F.; Frasier, T.R.; Whitehead, H. Using photography to determine sex in pilot whales (*Globicephala melas*) is not possible: Males and females have similar dorsal fins. *Mar. Mammal Sci.* **2013**, *29*, 213–220. [CrossRef]

90. Arranz, P.; de Soto, N.A.; Madsen, P.T.; Sprogis, K.R. Whale-watch vessel noise levels with applications to whale-watching guidelines and conservation. *Mar. Policy* **2021**, *134*, 104776. [CrossRef]

91. Carrillo, M.; Ritter, F. Increasing numbers of ship strikes in the Canary Islands: Proposals for immediate action to reduce risk of vessel-whale collisions. *J. Cetacacean. Res. Manag.* **2010**, *11*, 131–138.

92. De stephanis, R.; Urkiola, E. *Collisions between Ships and Cetaceans in Spain*; International Whaling Commission Scientific Committee SC/58/BC5; International Whaling Commission Scientific Committee: Munich, Germany, 2006; p. 6.

93. Sprogis, K.R.; Videsen, S.; Madsen, P.T. Vessel noise levels drive behavioural responses of humpback whales with implications for whale-watching. *eLife* **2020**, *9*, e56760. [CrossRef]

94. Booth, C.G.; Sinclair, R.R.; Harwood, J. Methods for Monitoring for the Population Consequences of Disturbance in Marine Mammals: A Review. *Front. Mar. Sci.* **2020**, *7*, 115. [CrossRef]

95. Bejder, L.; Samuels, A.; Whitehead, H.; Gales, N.; Mann, J.; Connor, R.; Heithaus, M.; Watson-Capps, J.; Flaherty, C.; Krützen, M. Decline in Relative Abundance of Bottlenose Dolphins Exposed to Long-Term Disturbance. *Conserv. Biol.* **2006**, *20*, 1791–1798. [CrossRef] [PubMed]

96. Lusseau, D.; Slooten, E.; Currey, R. Unsustainable Dolphin-watching Tourism in Fiordland, New Zealand. *Tour. Mar. Environ.* **2006**, *3*, 173–178. [CrossRef]